Electron energy-band structures of some AgCd alloys

N. C. Debnath,* M. Roychowdhury, and S. Chatterjee

Department of General Physics and X-rays, Indian Association for the Cultivation of Science, Calcutta 700032, India

(Received 6 September 1978; revised manuscript received 9 May 1979)

Complex energy-band structures of AgCd alloys have been determined by the alloy–Koringa-Kohn-Rostoker-Ziman (KKRZ) method for two different concentrations, and the optical properties estimated from these calculations have been compared with experiment. On the low-concentration side agreement with experiment is found to be excellent, whereas on the higher-concentration end a slight deviation is observed. This is probably due to the fact that the average-T-matrix approximation, which is the basis of the alloy-KKRZ method, is more suited for relatively lower concentrations of the alloying material. An effect of the charge transfer on the higher-concentration alloys has also been investigated. The results show that the disagreement with the experiment can also be accounted for by the charge-transfer effect.

I. INTRODUCTION

In recent years a lot of work[1-5] has been done theoretically on the electronic energy bands and optical properties of alloys mainly through one- and two-band models. The essential feature of these works is that they utilize the single-site approximation of the multiple-scattering theory of Lax[6] to approximate the t matrix of the system via the coherent potential approximation[7,8] (CPA) or the average-T-matrix approximation (ATA).[9,10] Because of its self-consistent nature the CPA has been used more widely than the ATA. Although the CPA is known to be more accurate it has not been possible to apply it to actual solids which cannot be described by one or two tight-binding model bands. These model calculations have been able to explain many of the beautiful features of the density of states and optical spectra qualitatively. Many authors[1] even showed from the model calculation that the ATA is the zeroth-order solution of the self-consistent CPA and hence for lower concentration of the alloying materials the ATA, which is much simpler than the CPA from a computational viewpoint, may describe the alloy fairly well.

But with the advent of the seventies it was felt that the models used in earlier calculations were very idealized cases of actual solids and hence they were not able to explain details of the various electronic properties of actual solids. So an attempt was made by Soven[11] to describe the CPA in terms of actual muffin-tin potentials. But even after Gyorffy[12] put Soven's idea in a more practical form it still could not be applied to actual solids. Recently, however, a number of authors[13] have claimed to have solved the CPA for a muffin-tin-potential model of the solid. These authors have been able to solve only for density of states and joint density of states but other details such as

Fermi surface could not be obtained from this theory. This could only come from the spectral density function, obtaining such details from a (complex) E-$\vec{k}$ relation in a further approximation. Moreover, since the theory of the crystalline substances are all described in terms of the E-$\vec{k}$ dispersion relation, one would be very much tempted to describe the alloy problem still in terms of the crystalline theory, though modified in some sense.

The difficulty in finding out the E-$\vec{k}$ relations for the binary alloys stems from the destruction of the periodicity of the alloy which makes the wave vector $\vec{k}$ no longer a good quantum number. But in the case of substitutional alloys the position of the atoms does not change, rather the different alloying atoms are randomly distributed in an otherwise empty periodic lattice. Since the CPA and ATA both depend on the effective medium, the only difference is that a complex potential arising out of the CPA condition is put at each lattice point of the periodic crystal in the former case, whereas an average t matrix is put at each periodic lattice point in place of the t matrix of the individual scatterer in the latter case. The description of the electronic properties of substitutional alloys can still be made through the conventional E-$\vec{k}$ relation. But the value of the energy coming out of the secular determinant in the angular momentum representation in either case would be complex having a small imaginary part, which may now be interpreted as the lifetime broadening of the energy states. The complex nature of the energy is apparent for both the CPA and ATA because in both cases the effective scattering amplitude $f_l = -\sqrt{E}\,T_l$ can be parametrized as $f_l = (1/2i) \times (\alpha_l e^{2i\delta_l} - 1)$ with $\alpha_l < 1$ as compared to $\alpha_l = 1$ for the crystalline case, since for $\alpha_l = 1$ the imaginary part from f_l cancels exactly with the imaginary part of the structural Green function. In the case of the CPA, the equation determining the energy

is a matrix equation and if one takes at least up to $l = 2$, one needs to solve a matrix equation of at least order 9 self-consistently. This is a very complicated numerical problem. On the other hand one gets the usual secular determinant in the case of the ATA; only the matrix elements have now to be calculated in complex numbers and hence the solution of the secular determinant will now be only slightly more difficult for this case than the usual Korringa-Kohn-Rostoker (KKR) calculation of crystalline solids. However, it should be mentioned, as has been pointed out by Bansil et al.,[14] the complex energy bands do not contain enough information for the average electronic density of states, although Schwartz and Bansil[15] have derived the ATA spectral density $G(\vec{k}, E)$ from which the average density of states $\langle \rho(E) \rangle$ can be obtained by integration over all $\vec{k}$ in the Brillouin zone (BZ).

The application of the ATA in KKR theory and the subsequent study of some alloys by Bansil et al[14, 16] were done in the angular momentum representation. There is, however, an alternative plane-wave representation of the KKR method by Ziman,[17] known as the Korringa-Kohn-Rostoker-Ziman (KKRZ) method which is very easy to adopt for computational purpose because of the pseudopotential nature of the secular determinant. The Fourier transform of the pseudopotential contains the lth angular momentum component of the free-electron Green's function and the inverse of the lth angular momentum component of the t matrix of the individual scatterers. The imaginary parts of these two lth angular momentum components are equal and opposite, and hence they cancel each other keeping the secular equation real. However, if with the stipulation of Bansil et al.[14, 16] we replace the angular momentum components of the t matrix by their configurational averages, the imaginary parts in the secular determinant will no longer cancel and hence the l-dependent pseudopotential will now be complex. The idea, although pointed out by Bansil et al.[14, 16] and utilized by Debnath and Chatterjee[18] to compute complex energy bands and optical spectra of some Mg alloys, may be very suitable for more complex systems such as the alloys of the noble metals for which some experimental results exist.

Recently there has been a number of experimental works on the optical spectra of some binary alloys, of which the work of Flaten and Stern[19] on some silver alloys are notable. In this work we apply the KKRZ method with the ATA to compute the complex energy bands of two compositions of AgCd alloys throughout the BZ. We then use these data to interpret the optical absorption of Flaten and Stern.[19]

II. OUTLINE OF THE METHOD

The Kohn-Rostoker[20] secular determinant as derived from the multiple-scattering theory[21] can be written in terms of the lth angular momentum component of the t matrix of the individual scatterers as

$$\det \| G'_{LL'}(k) - (T^j_l)^{-1} \delta_{LL'} \| = 0 , \qquad (1)$$

where the incomplete Green's function $G'(k)$ differs from the complete Green's function $G(k)$ by a single propagator $\mathcal{G}_0$:

$$G'_k = G_k - \mathcal{G}_0 . \qquad (2)$$

The complete Green's function is given by

$$G(r, r') = \sum_n \frac{e^{i(\vec{k} + \vec{k}_n) \cdot (\vec{r} - \vec{r}')}}{E - |\vec{k} + \vec{K}_n|^2} \delta_{nn'} . \qquad (3)$$

The lth angular momentum components of T^j_l and $\mathcal{G}_0$ are given by

$$(T^j_l)^{-1} = -\kappa \cot \eta^j_l + i\kappa , \qquad (4)$$

$$(\mathcal{G}_0)_{LL'} = \kappa \{ [n_l(\kappa r)/j_l(\kappa r)] - i \} \delta_{LL'} , \qquad (5)$$

where $\kappa = \sqrt{E}$. Bansil et al.[14, 16] replaced T^j_l given by (4) with the configurational average given by

$$\langle T_l \rangle = C T^A_l + (1 - C) T^B_l , \qquad (6)$$

where C is the concentration and A, B are the alloying materials. Thus following Ziman[17] we consider Eq. (1) as the singularity condition of the operator $\langle T \rangle^{-1} - G'$, which may be written as

$$\langle T \rangle^{-1} - G' = \langle T \rangle^{-1} + \mathcal{G}_0 - G$$
$$= \Omega G \{ (1/\Omega) G^{-1} - (1/\Omega)(\langle T \rangle^{-1} + \mathcal{G}_0)^{-1} \}$$
$$\times (\langle T \rangle^{-1} + \mathcal{G}_0). \qquad (7)$$

Singularities of the Green's function of the system may be thought to arise from the zeros of the matrix

$$[(1/\Omega) G^{-1} - (1/\Omega)(\langle T \rangle^{-1} + \mathcal{G}_0)^{-1}] = \frac{1}{\Omega} G^{-1} - \Gamma . \qquad (8)$$

If we now take the plane-wave representation of the operator (8) we have the secular determinant, since

$$\langle n | G | n' \rangle = \frac{1}{E - |\vec{k} + \vec{K}_n|^2} \delta_{nn'} , \qquad (9)$$

$$\det \| (E - |\vec{k} + \vec{K}_n|^2) \delta_{nn'} - \Gamma_{nn'} \| = 0 ,$$

and Γ appears to be the effective potential of the system. We will now show that whenever the concentration C is different from 0 and 1, $\Gamma_{nn'}$ is complex. To do this we write the expression for $\Gamma_{nn'}$ as

$$\Gamma_{nn'} = \int \int \Gamma(r, r') e^{i\vec{k}_n \cdot \vec{r}} e^{-i\vec{k}_{n'} \cdot \vec{r}'} d\vec{r} \, d\vec{r}'$$

$$= \frac{1}{(4\pi)^2} \sum_{LL'} \int \int \Gamma(r, r') j_l(k_n r) j_{l'}(k_n r') r^2 \, dr \, r'^2 \, dr' \, Y_L(\hat{r}) Y_{L'}(\hat{r}') d\Omega \, d\Omega'$$

$$= (4\pi)^2 \sum_L \int \int \Gamma_l(r, r') j_l(k_n r) j_l(k_n r') r^2 dr \, r'^2 \, dr'$$

$$= (4\pi)^2 \sum_L \Gamma_l(\kappa, \kappa) \frac{j_l(k_n R_i) j_l(k_{n'} R_i)}{j_l^2(\kappa R_i)} \quad ,$$

assuming $\Gamma_l(r, r') = A\delta(r - R_i)\delta(r' - R_i)$, R_i being the muffin-tin radius. Finally we have

$$\Gamma_{nn'} = 4\pi \sum_L (2l+1) \frac{\Gamma_l(\kappa, \kappa') j_l(k_n R_i) j_l(k_{n'} R_i)}{j_l^2(\kappa R_i)}$$

$$\times P_l(\cos\theta_{nn'}), \tag{10}$$

where

$$\Gamma_l(\kappa, \kappa') = (1/\Omega)[\langle T_l \rangle^{-1} + (\mathcal{G}_0)_l]^{-1}$$

$$= \frac{1}{\Omega}\left[\langle T_l \rangle^{-1} + \kappa\left(\frac{n_l(\kappa R_i)}{j_l(\kappa R_i)} - i\right)\right]^{-1}, \tag{11}$$

$$\langle T_l \rangle = \frac{C}{-\kappa \cot\eta_l^A + i\kappa} + \frac{1-C}{-\kappa \cot\eta_l^B + i\kappa} \quad . \tag{12}$$

Thus from (11) and (12) it is evident that imaginary parts from $\langle T_l \rangle^{-1}$ and $(\mathcal{G}_0)_l$ will not cancel for any value of C other than 0 or 1, which is the case of the pure crystal consisting of either A or B atoms. The phase shift η_l is given in terms of the logarithmic derivative L_l as

$$\cot\eta_l = \frac{n_l'(\kappa R_i) - n_l(\kappa R_i)L_l}{j_l'(\kappa R_i) - j_l(\kappa R_i)L_l} \quad . \tag{13}$$

Thus by combining (13), (12), (10), and (9) one can easily find out the complex band structure throughout the BZ.

III. RESULTS AND DISCUSSIONS

In order to calculate the complex energy bands of AgCd one would require a proper crystal potential. For pure Ag there are a number of band-structure calculations assuming various types of potentials of which the "universal potential" of Gasper was found to be very suitable in explaining the experimentally observed properties of the pure metal.[22, 23] The expression for the potential is given by

$$V(r) = -\frac{2Z}{r} \frac{\exp(-0.1837x)}{1+1.05x} - 2Z \frac{C'\exp(-0.04x)}{1+9x},$$
$$\tag{14}$$

where $x = rZ^{1/3}/0.88534$, Z is the nuclear charge, and $C' = 3.053/Z^{1/3}$. This potential, although ini-

tially put forward for atoms, was used by Ballinger and Marshall[23] to construct the crystal potential in their calculation of band structure of Ag. By making the constant C' a variable, they calculated the Fermi surface of Ag from the band-structure data and could get a very good fit with the experiment for $C' = 3.053/Z^{1/3}$. For this reason we have utilized this potential to calculate the logarithmic derivative of both Ag and Cd atoms constituting the alloys by the Numerov method. The muffin-tin constants have been found by the method described by Loucks.[24] The muffin-tin constant for the alloy is then determined from the following relation:

$$V_0^{\text{alloy}} = CV_0^A + (1-C)V_0^B. \tag{15}$$

For all energies it was found that the quantity Γ_l appearing in Eq. (10) becomes negligible for $l > 4$ and hence we have kept terms up to $l = 4$ in Eq. (10).

The results of the complex band structure of AgCd alloy for 23 at.% and 40 at.% Cd are plotted in Figs. 1 and 2, respectively, and the energy values at the highest symmetry points are given in Table I. The imaginary parts of energy values are shown in the figures as shading over the real energy values after multiplication of suitable factors. The Cd $4d$ bands have been separated from the $4d$ bands of Ag as has been the case of CuZn system shown by Bansil et al.[14] Following these authors we have calculated the Fermi surface by filling the pure Ag band structure with $11C + 12(1 - C) = 12 - C$ electrons per atom. This assumption has to be made in order to accomodate more filled electrons in the Cd bands than in the Ag bands. This automatically pushes the Fermi level up with the increase of Cd concentration, and the effect of this increase is already noted in the experimental optical spectra obtained by Flaten and Stern[19] as shown in Fig. 3, where the three curves of the ϵ_2 spectra corresponds to 2, 23, and 40 at.% Cd concentrations. If we make a comparative study of these three curves we see that the alloy with 2 at.% concentration Cd, which represents more or less the pure Ag case, contains one peak near 4 eV and
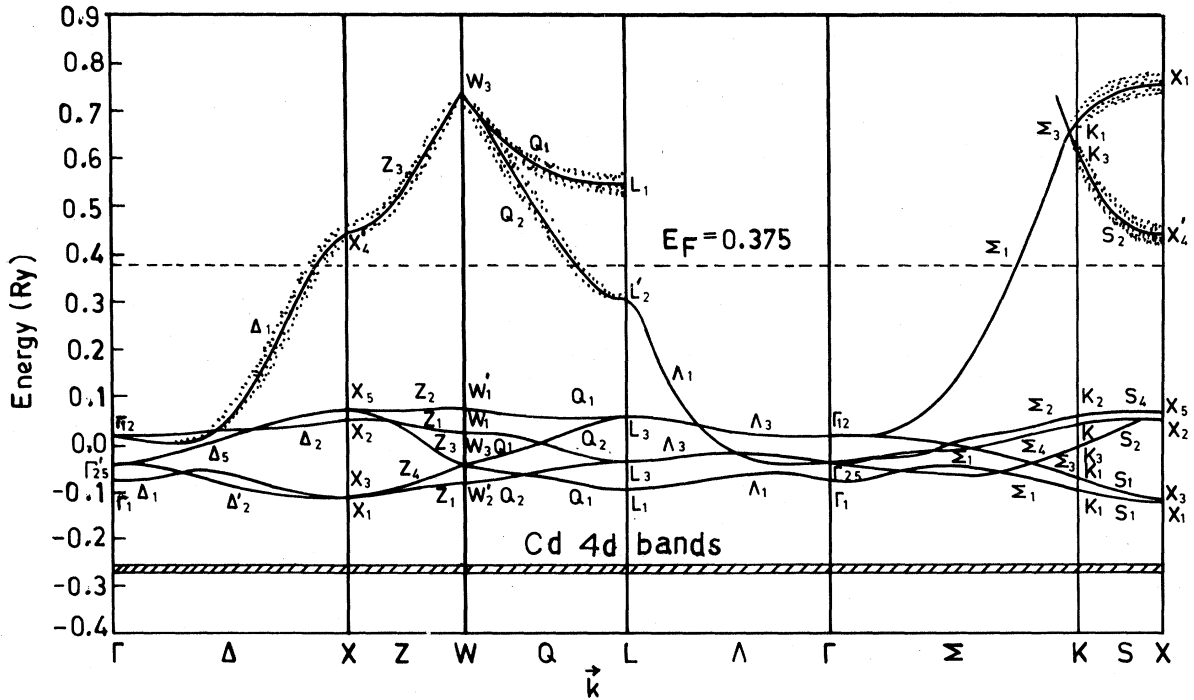
FIG. 1. Complex energy bands for Ag_xCd_{1-x}, $x = 0.77$. The shading of the bands corresponds to ten times the imaginary part of the complex energies.
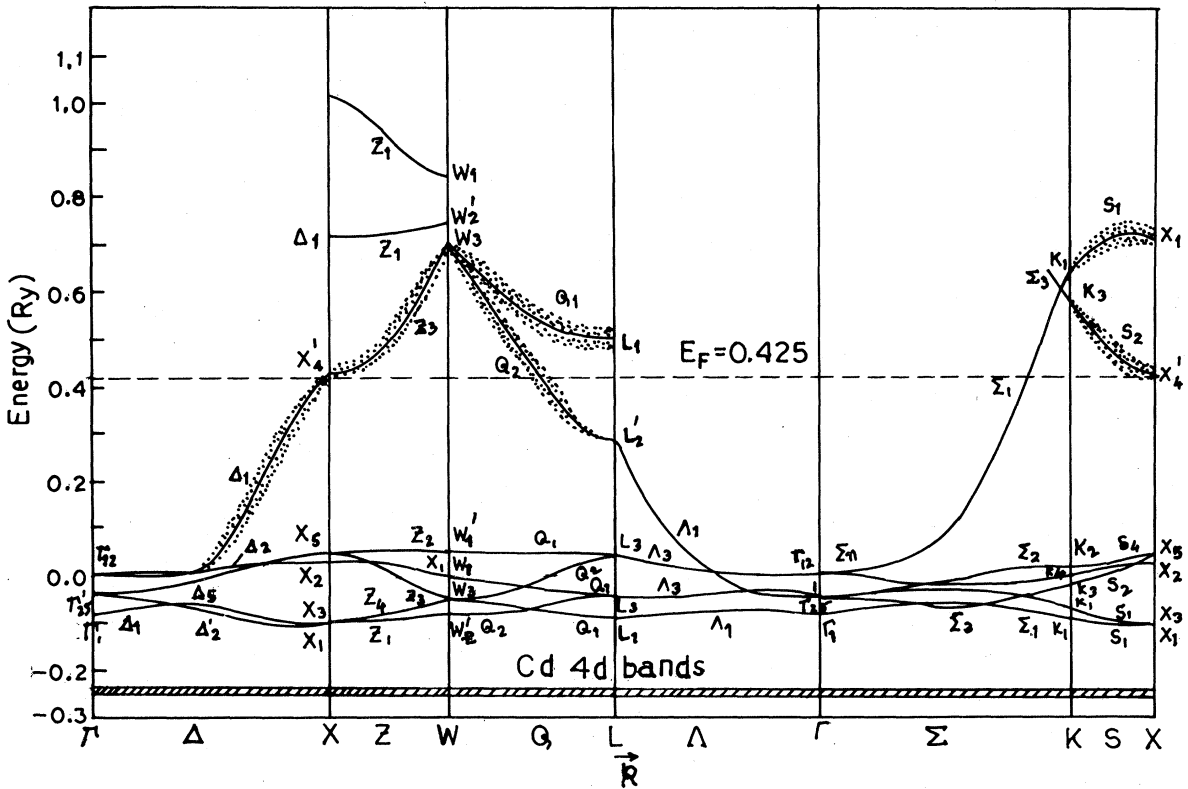
FIG. 2. Complex energy bands for Ag_xCd_{1-x} ($x = 0.6$) without shifting the muffin-tin constant. The shading of the bands corresponds to eight times the imaginary part of the complex energies.

TABLE I. Complex energy values in Ry for $Ag_x Cd_{1-x}$ alloy. The real and the imaginary parts of the complex energy are shown in the parentheses in each column.

Symmetry	$Ag_{0.77}Cd_{0.23}$	$Ag_{0.6}Cd_{0.4}$	$Ag_{0.6}Cd_{0.4}$ (muffin–tin constant of Ag shifted by 0.1 Ry for $l = 2$)	$Ag_{0.6}Cd_{0.4}$ (muffin–tin constant of Ag shifted by 0.2 Ry for $l = 2$)
Γ_1	(−0.078 39, −0.001 59)	(−0.082 21, −0.001 46)	(−0.089 85, −0.001 51)	(−0.161 65, −0.001 42)
Γ_{25}'	(−0.044 57, −0.000 4)	(−0.048 45, −0.000 11)	(−0.080 39, −0.000 60)	(−0.157 78, −0.001 77)
Γ_{12}	(0.018 81, 0.0)	(0.005 31, 0.0)	(−0.047 89, −0.000 08)	(−0.106 45, −0.000 32)
X_1	(−0.113 26, −0.000 61)	(−0.102 67, −0.000 89)	(−0.152 95, −0.001 91)	(−0.209 77, −0.003 81)
X_3	(−0.111 21, −0.000 57)	(−0.097 41, −0.000 74)	(−0.148 23, −0.001 78)	(−0.201 58, −0.003 12)
X_2	(0.048 36, −0.000 04)	(0.039 85, −0.000 06)	(−0.023 52, −0.000 02)	(−0.076 20, −0.000 38)
X_5	(0.070 14, −0.000 12)	(0.049 40, −0.000 14)	(−0.004 11, 0.0)	(−0.066 17, −0.000 18)
X_4'	(0.444 36, −0.002 87)	(0.423 46, −0.004 02)	(0.451 39, −0.003 54)	(0.442 19, −0.000 50)
L_1	(−0.094 88, −0.000 55)	(−0.090 75, −0.000 74)	(−0.122 54, −0.001 05)	(−0.181 33, −0.002 24)
L_3	(−0.036 88, −0.000 03)	(−0.042 44, −0.000 88)	(−0.089 81, −0.000 45)	(−0.158 69, −0.001 36)
L_3	(0.063 26, −0.000 08)	(0.040 31, −0.000 05)	(−0.010 95, 0.0)	(−0.072 50, −0.000 16)
L_2'	(0.304 17, −0.002 70)	(0.285 43, −0.002 66)	(0.297 97, −0.003 12)	(0.298 30, −0.002 84)
L_1	(0.547 20, −0.004 64)	(0.508 19, 0.006 59)	(0.498 81, −0.005 73)	(0.482 82, −0.006 05)

with alloying, this peak splits into two peaks—one decreasing, the other increasing as the concentration of Cd. Hence the electron per atom ratio increases, the major peak being shifted towards the lower photon energy sides. As pointed out by previous workers[25] and also by Flaten and Stern[19] this behavior can be understood from Figs. 1 and 2 of complex band structure for 23 and 40 at. % Cd. It is evident from the trend of the band structure that for the pure case as has been shown by Ballinger and Marshall[23] the Fermi level lies just above the L_2' level and optical transitions are then mainly from the Q axis near L point and Δ axis near the X point. Since the transitions from both these points involve more or less the same energy, these transitions give a single peak near 4 eV. But as the concentration of Cd increases the number of electron per atom ratio increases and the Fermi energy also increases. The pushing up of the Fermi level coupled with the change of the band structure due to alloying has a remarkable
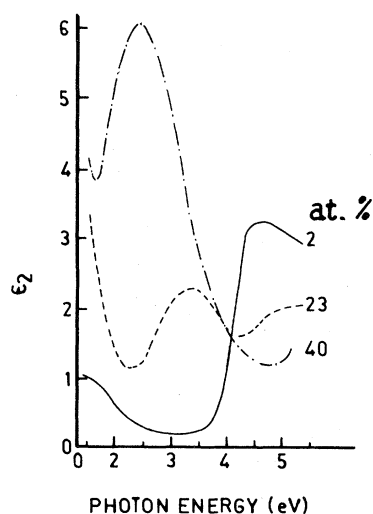
FIG. 3. Experimental results of the imaginary part of the dielectric constant ϵ_2 for $Ag_x Cd_{1-x}$ ($x = 0.98$, 0.77, and 0.60).

effect in the sense that the transition energies be-
tween the bands in the Q axis and in the Δ axis
are different, indicating two different peaks at
different energies instead of the one peak for the
pure Ag. This phenomenon, which is also appa-
rent from the experimental ϵ_2 spectra, may be
looked upon as a splitting of the peak at 4 eV for
pure Ag into two peaks, one in the lower-energy
side and the other in the increasing-energy side.
Since the joint density of states, which is respon-
sible for the peaks in the optical transition, will
be highest in the flatter regions of the bands, the
peaks from the theoretical band-structure curves
are estimated to be at 5.03 and 3.28 eV for the
alloy of 23 at.% Cd and at 5.30 and 2.87 eV for the
alloy of 40 at.% Cd. These two peaks involve
transitions in the Δ axis near x_5 and x_4' and Q axis
near L_2' and L_1. Comparing with experimental
values for the 23-at.% Cd alloy where the peaks
occur at 3.33 and 5.10 eV we find a very good
agreement between the theory and experiment.
However, for the 40-at.% Cd alloy there is a
deviation of our theoretical results from the ex-
perimental peak. The experimental peak at the

lower-energy side occurs at 2.37 eV and the theo-
retical value deviates from this by 0.5 eV. The
higher peak for the experimental spectra is defi-
nitely outside 6 eV. This small deviation,
especially for the low-energy side peak, may be
attributed to the decoupling assumption made in
the formalism of the ATA, which seems to be
more accurate for the relatively lower concen-
tration of the alloying.

Finally, we study the effect of charge transfer.
The problem of charge transfer has been dealt
with by many authors.[14,26,27] There are mainly
two models for charge transfer studies, namely,
the charge-renormalization (CR) model and the
shifted-muffin-tin (SMT) model. We have, how-
ever, employed the SMT model for studying the
charge transfer. Since the experimental spectra
for the lower concentration of Cd (23 at.%) agree
with the theoretical results very well we study the
effect only for the alloy with Cd concentration of
40 at.%. Here following Bansil $et\ al.$[14] we change
the muffin-tin constant for $l=2$ for Ag by 0.1 and
0.2 Ry. The complex band structure obtained with
these changes is shown in Figs. 4 and 5. From
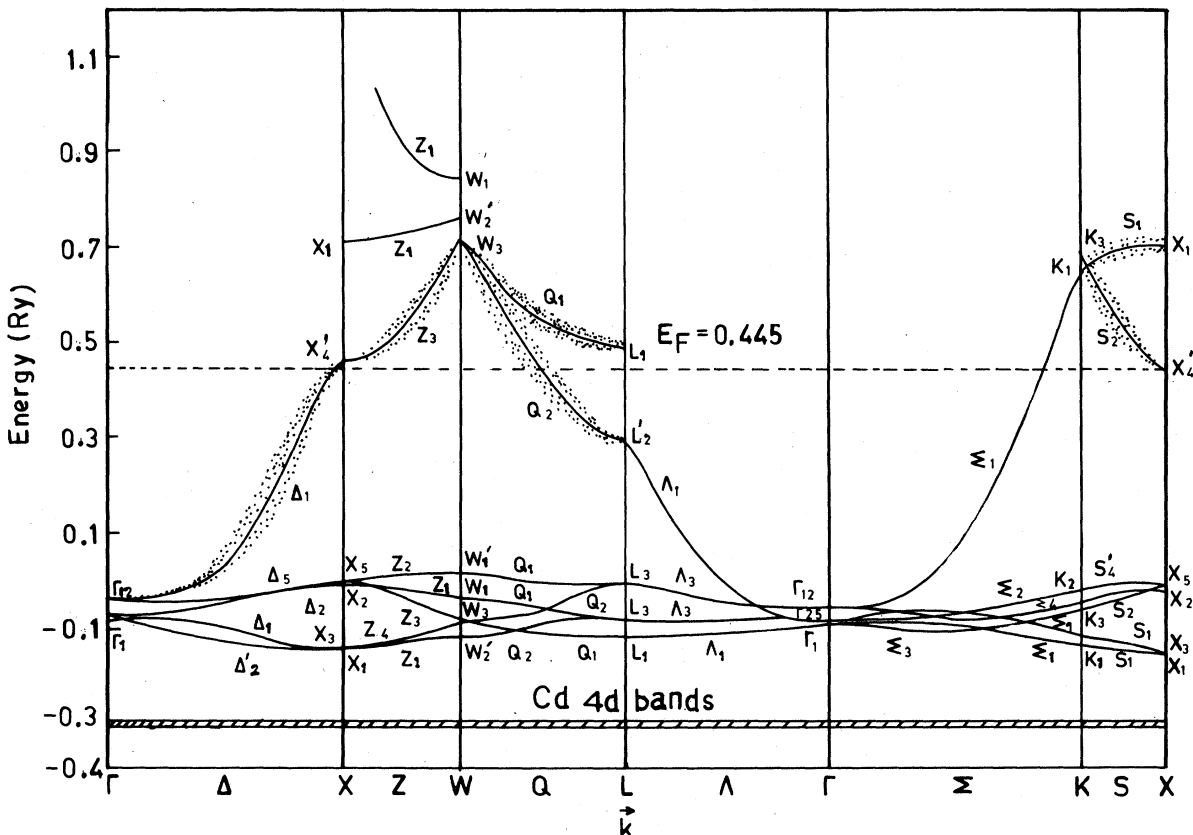
FIG. 4. Complex energy bands for Ag_xCd_{1-x} ($x=0.6$) with the muffin-tin constant of Ag shifted by an amount 0.1 Ry for $l=2$. The shading of the bands corresponds to eight times the imaginary part of the complex energies.
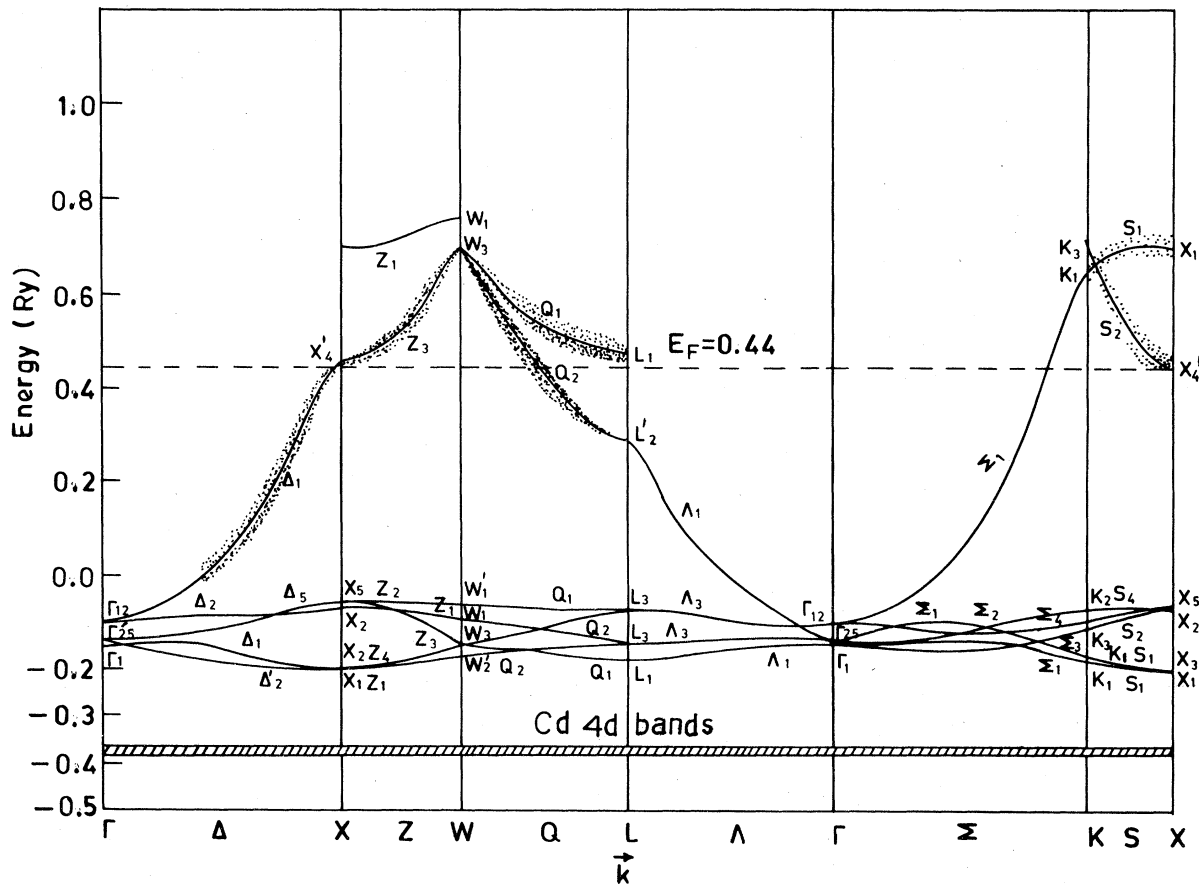
FIG. 5. Complex energy bands for Ag_xCd_{1-x} ($x = 0.6$) with the muffin-tin constant of Ag shifted by an amount 0.2 Ry for $l = 2$. The shading of the bands corresponds to eight times the imaginary part of the complex energies.

these figures a similar analysis puts the possible energies of the two peaks at 2.64 and 6.12 eV for the case of Fig. 4 and 2.48 and 6.66 eV for Fig. 5. The latter pair of values, especially the peak at 2.48 eV, now agrees more closely with the experiment. Thus considering charge transfer through the SMT model, the theoretical values can be made more agreeable with the experi-ments.

The experimental study of the Fermi surfaces of substitutional alloys have not yet been taken up in detail, probably because the Fermi surfaces are not well defined in the case of substitutional alloys owing to the breakdown of the periodic symmetry. Since the imaginary parts in the energy, which are the measure of the degree of disorder,
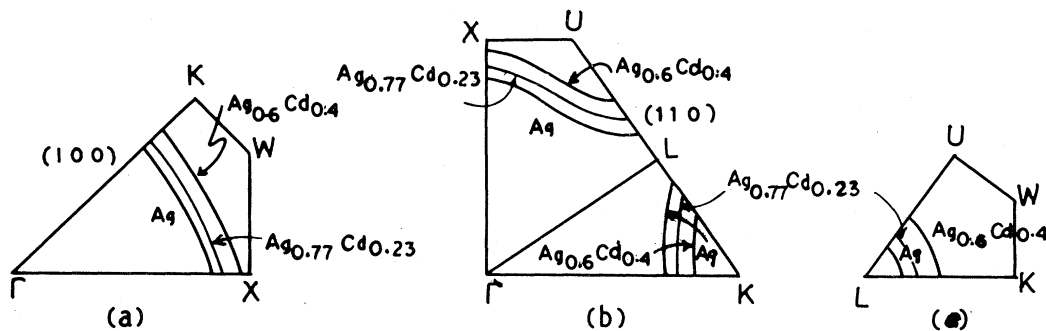
FIG. 6. Intersections of the Fermi surface of Ag and $Ag_{0.6}Cd_{0.4}$: (a) with a (100) plane, (b) with a (110) plane, and (c) with the hexagonal face of the Brillouin zone for the SMT model.

TABLE II. Fermi-surface properties of Ag_xCd_{1-x} alloys. The belly radii k_{100} and k_{110} and the neck radii k_N are given in units of $(2\pi/a)$, where a is the cube edge of the fcc AgCd alloy lattice.

Fermi-surface radii	Ag	$Ag_{0.6}Cd_{0.4}$	$Ag_{0.6}Cd_{0.4}$ (Muffin-tin constant for Ag shifted by 0.1 for $l=2$)	$Ag_{0.6}Cd_{0.4}$ (Muffin-tin constant for Ag shifted by 0.2 for $l=2$)
k_{100}	0.825	0.960	0.982	0.965
k_{110}	0.745	0.865	0.905	0.868
k_N	0.138	0.305	0.365	0.342

are not large, one may still define the Fermi surface in the virtual crystal with complex energy as has been done by Bansil et al.[14,16] These surfaces will not be sharp and will have uncertainty in a range of energy determined by the imaginary parts. Since the experimental study of Fermi surfaces of alloys have already been started,[28-31] we have also calculated the Fermi surfaces of these two alloys. They are shown in Fig. 6. Table II gives the Fermi-surface dimensions. As the imaginary parts are very small we have not shown the imaginary parts in this figure. Of the few experimental information about the neck and belly radii for the AgCd alloys the experiment of Tracy and Stern[30] may be worth mentioning. They have used the polar-reflection Faraday effect to calculate the ratio of the neck radius to the radius of the free-electron Fermi-surface sphere, and these are shown in Fig. 7 along with the belly radii as a function of the electron per atom ratio. The results from our calculation as well as the results of Halse model[32] calculation, also quoted by Tracy and Stern,[30] are also shown in the figure. From this figure it can be seen that our results are closer to the experiment for the higher concentration than the results of the Halse model calculation for the same concentration.

In this work we have tried to give an account of the electronic properties of the AgCd alloys from the ATA point of view. One may, however, point out that in the case of alloys it is better to use the CPA. But since the substitutional alloys retain[33] the periodic lattice corresponding to the virtual crystal, one may be tempted to describe the electronic properties of the alloys in terms of the periodic virtual-crystal lattice. As mentioned in the Introduction this type of calculation is not yet possible with the CPA, although Stocks et al.[13] have been able to calculate the density of states and optical spectra directly with muffin-tin potential in the CPA. However, a comparative study of the ATA and the CPA has been made by

Schwartz et al.[1] and the numerical aspects of the two approximations by Chen.[34] From these discussions it was concluded that the ATA may be viewed as the first iteration toward self-consistency, i.e., the CPA. In fact from the model calculation it has been shown that for large values of δ (Ref. 8) and concentration C the ATA density of states differs markedly from that of the CPA. An iterative averaged T-matrix approximation (IATA) was suggested by Chen[34] which converges from the virtual-crystal limit towards the CPA for all alloy parameters and for all energies inside the CPA bands. It is easy to do this for model bands but is probably very difficult at this stage with the alloy-KKRZ method which we have utilized in this work but may be persued in future.

In conclusion, we want to point out that for the lower concentration the optical spectra agree very well with the experiment, which may be due to the lower concentration of the alloying material. But since the results for the higher concentration do not agree exactly, we may think that this may be due to two reasons, (1) charge transfer and (2) the approximate nature of ATA. But since the results
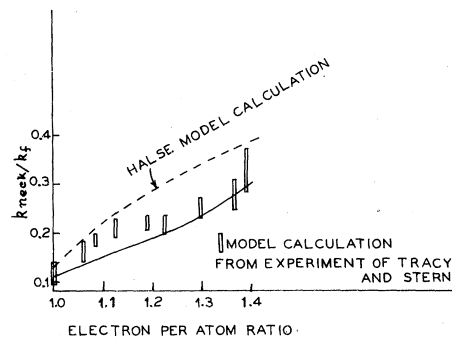
FIG. 7. Ratio of the neck radii to the ratio of the free-electron sphere. Bars and the solid line denote the experimental results, and the theoretical results from this calculation, respectively, while the dashed line is from the Halse model calculation.

with the shifted muffin tin can be made to agree with the experiment, one may conclude that in this concentration the charge transfer is more important.

---

*Present address: Materials Science Laboratory, Corporate Research Development Division, Bharat Heavy Electricals Ltd., Vikasnagar, Hyderabad 500 593, India.

[1] L. Schwartz and H. Ehrenreich, Ann. Phys. (N.Y.) 64, 100 (1971).

[2] R. J. Elliott, J. A. Krumhausl, and P. L. Leath, Rev. Mod. Phys. 46, 465 (1974).

[3] S. Kirkpatrick, B. Velicky, and H. Ehrenreich, Phys. Rev. B 1, 3350 (1970).

[4] G. M. Stocks, R. W. Williams, and J. S. Faulkner, Phys. Rev. B 4, 4390 (1971).

[5] K. Levin and H. Ehrenreich, Phys. Rev. B 3, 4172 (1971); C. D. Gelatt, Jr. and H. Ehrenreich, ibid. 10, 398 (1974).

[6] M. Lax, Rev. Mod. Phys. 23, 287 (1951).

[7] P. Soven, Phys. Rev. 156, 809 (1967).

[8] B. Velicky, S. Kirkpatrick, and H. Ehrenreich, Phys. Rev. 175, 747 (1968).

[9] J. Korringa, J. Phys. Chem. Solids 7, 252 (1958).

[10] J. L. Beeby, Proc. R. Soc. London, Ser. A 302, 113 (1967).

[11] P. Soven, Phys. Rev. B 2, 4715 (1970).

[12] B. L. Gyorffy, Phys. Rev. B 5, 2382 (1972).

[13] G. M. Stocks, W. M. Temmerman, and B. L. Gyorffy, Phys. Rev. Lett. 41, 339 (1978); G. M. Stocks, B. L. Gyorffy, E. S. Giuliano, and R. Ruggeri, J. Phys. F 7, 1859 (1977); A. Bansil, Phys. Rev. Lett. 41, 1670 (1978); W. M. Temmerman, B. L. Gyorffy, and G. M. Stocks, J. Phys. F 8, 2461 (1978); J. Kanamori, H. Akai, N. Hamada, and H. Miwa, Physica 91, B153 (1977).

[14] A. Bansil, H. Ehrenreich, L. Schwartz, and R. E. Watson, Phys. Rev. B 9, 445 (1974).

[15] L. Schwartz and A. Bansil, Phys. Rev. B 10, 3261 (1974).

[16] A. Bansil, J. Schwartz, and H. Ehrenreich, Phys. Rev. B 12, 2893 (1975).

[17] J. M. Ziman, Proc. Phys. Soc. London 86, 337 (1965); J. M. Ziman, Solid State Phys. 26, 1 (1971).

[18] N. C. Debnath and S. Chatterjee, J. Phys. C 11, 3403 (1978).

[19] C. J. Flaten and E. A. Stern, Phys. Rev. B 11, 638 (1975).

[20] W. Kohn and N. Rostoker, Phys. Rev. 94, 1111 (1954).

[21] J. L. Beeby, Proc. R. Soc. London Ser. A 279, 82 (1964); J. Korringa, Physica 13, 392 (1947).

[22] S. Chatterjee and S. K. Sen, Proc. Phys. Soc. London 87, 779 (1966).

[23] R. A. Ballinger and C. A. W. Marshall, J. Phys. C 2, 1822 (1969).

[24] T. L. Loucks, Augmented Plane Wave Method (Benjamin, New York, 1967).

[25] F. M. Mueller and J. C. Phillips, Phys. Rev. 157, 600 (1967); C. Y. Fong, M. L. Cohen, R. R. L. Zucca, J. Stokes, and Y. R. Shen, Phys. Lett. 25, 1486 (1970).

[26] K. Levin and H. Ehrenreich, Phys. Rev. B 3, 4172 (1971); F. Brouers and A. V. Velyayev, ibid. 5, 348 (1972); C. D. Gelatt and H. Ehrenreich, Bull. Am. Phys. Soc. 18, 94 (1973).

[27] E. A. Stern, Phys. Rev. 144, 545 (1966); Phys. Rev. B 1, 1518 (1970); Phys. Rev. Lett. 26, 1630 (1971); A. R. Miedema, F. R. De Boer, and P. F. de Chatel, J. Phys. F 3, 1558 (1973).

[28] W. Triftshauser and A. T. Stewart, J. Chem. Phys. Solids 2, 2717 (1971); L. J. Hornbeck, W. K. Fung, and W. L. Gordon, Phys. Rev. B 15, 4750 (1977).

[29] S. Berko and J. Mader, Appl. Phys. 5, 287 (1975); Proceedings of the International Conference of Electron Lifetimes in Metals [Phys. Condens. Matter 19, 404 (1975)].

[30] J. M. Tracy and E. A. Stern, Phys. Rev. B 8, 582 (1973).

[31] E. A. Stern, in Charge Transfer/Electronic Structure of Alloys, edited by R. Willens and L. Bennett (Metallurgical Society of AIME, New York, 1974), pp. 197–222.

[32] M. R. Halse, Philos. Trans. R. Soc. London Ser. A 265, 507 (1969).

[33] H. Ehrenreich and L. Schwartz, Solid State Phys. 31, 149 (1976).

[34] A. B. Chen, Phys. Rev. B 7, 2230 (1973).